

Sesamol Reduces the Atherogenicity of Electronegative L5 LDL *in Vivo* and *in Vitro*

Wei-Yu Chen,^{†,§,#} Fang-Yu Chen,^{‡,§,⊥,#} An-Sheng Lee,^{§,||} Kuan-Hsiang Ting,^{‡,§,∇} Chia-Ming Chang,^{‡,§} Jing-Fang Hsu,^{‡,§,○} Wei-Shine Lee,^{‡,§} Joen-Rong Sheu,[⊥] Chu-Huang Chen,^{*,§,○,□,◇} and Ming-Yi Shen^{*,‡,§,⊥}

[†]Graduate Institute of Basic Medical Science, [‡]Graduate Institute of Clinical Medical Science, and [∇]Department of Biological Science and Technology, College of Life Sciences, China Medical University, No. 91 Hsueh-Shih Road, Taichung 40402, Taiwan

[§]L5 Research Center, China Medical University Hospital, No. 2 Yude Road, Taichung 40447, Taiwan

[⊥]Department of Pharmacology, School of Medicine, College of Medicine, Taipei Medical University, No. 250 Wuxing Street, Taipei City 110, Taiwan

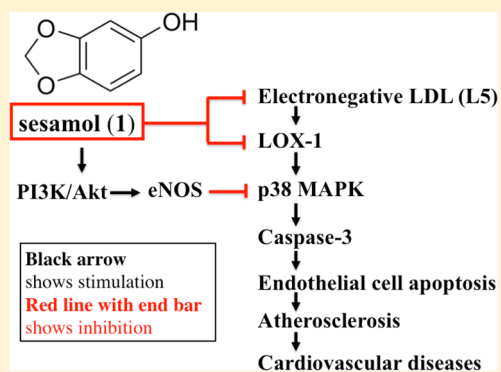
^{||}Department of Medicine, Mackay Medical College, New Taipei City 252, Taiwan

[○]Center for Lipid Biosciences, Kaohsiung Medical Hospital, Kaohsiung 807, Taiwan

[□]Vascular and Medicinal Research, Texas Heart Institute, 6770 Bertner Avenue, Houston, Texas 77030, United States

[◇]Section of Cardiovascular Research, Department of Medicine, Baylor College of Medicine, Houston, Texas 77030, United States

ABSTRACT: Highly electronegative low-density lipoprotein (LDL) L5 induces endothelial cell (EC) apoptosis, which leads to the development of atherosclerosis. We examined the effects of sesamol (**1**), a natural organic component of sesame oil, on plasma L5 levels and atherosclerosis development in a rodent model and on the L5-induced apoptosis of ECs. Syrian hamsters, which have an LDL profile similar to that of humans, were fed a normal chow diet (control), a high-fat diet (HFD), or a HFD supplemented with the administration of 50 or 100 mg/kg of **1** via oral gavage (HFD+**1**) for 16 weeks ($n = 8$ per group). Hamsters in the HFD+**1** groups had reduced plasma L5 levels when compared with the HFD group. Oil Red O staining showed that atherosclerotic lesion size was markedly reduced in the aortic arch of hamsters in the HFD+**1** groups when compared with that in the HFD group. In human aortic ECs, 0.3–3 μM **1** blocked L5-induced apoptosis in a dose-dependent manner. Further mechanistic studies showed that **1** inhibited the L5-induced lectin-like oxidized LDL receptor-1 (LOX-1)–dependent phosphorylation of p38 MAPK and activation of caspase-3 and increased phosphorylation of eNOS and Akt. Our findings suggest that sesamol (**1**) protects against atherosclerosis by reducing L5-induced atherogenicity.



Lipid-lowering agents are used to treat dyslipidemia such as hypercholesterolemia and to prevent the occurrence of cardiovascular diseases.¹ Statins are the most potent, well-tolerated, and widely used cholesterol-lowering agents, but their clinical use has been associated with acute liver injury and muscle toxicity.^{2,3} Thus, the identification of an alternative, safer lipid-lowering agent is of great clinical importance.

Phenolic compounds, which are widely present in plants, have recently received considerable attention because of their antioxidant properties and ability to reduce blood cholesterol levels.^{4,5} Sesamol (**1**), a derivative of phenol and a natural organic compound, is a component of sesame oil and is an antioxidant that may protect the body against damage from free radicals.^{6,7} In addition to its antioxidant activity, **1** has antimutagenic, antihepatotoxic, anti-inflammatory, antiaging, and antiplatelet properties.^{7–10} However, it is not known what effects **1** has on the development of atherosclerosis.

Atherosclerosis leads to a wide variety of cardiovascular diseases. The initiation and progression of atherosclerosis are

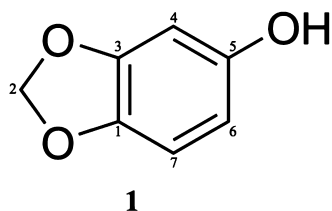
believed to involve damage to vascular endothelial cells (ECs) or the apoptosis of vascular ECs.^{11–14} Experimentally derived, oxidized low-density lipoprotein (oxLDL) is a modified form of LDL that exerts pro-atherogenic effects in ECs by inducing apoptosis.¹⁵ Notably, naturally occurring electronegative LDL has also been found to be pro-inflammatory and cytotoxic to cultured ECs.^{12,15} The most electronegative type of LDL, called L5, is a subfraction of LDL that can be isolated by the separation of LDL according to charge by using high-capacity anion-exchange chromatography.^{12,16} Plasma L5 levels have been shown to be elevated in patients with high cardiovascular risks such as hypercholesterolemia, type 2 diabetes mellitus, and smoking, as well as in patients with ST-elevation myocardial infarction (STEMI).^{12,17,18} In addition, the accumulation of L5 in blood vessels has been reported to be involved in

Received: September 26, 2014

Published: February 18, 2015

atherosclerosis and cardiovascular disease.^{19,20} Recently, we found that L5 isolated from patients with STEMI^{12,17} induced EC apoptosis by reducing the phosphorylation of Akt and inhibiting fibroblast growth factor 2 transcription via the lectin-like oxidized LDL receptor-1 (LOX-1) pathway.^{12,15,21} Thus, these findings have suggested that L5 participates in the progression of atherosclerosis by inducing EC apoptosis.

The purpose of this study was to investigate the effects of **1** on plasma L5 levels and the development of atherosclerosis in a rodent model and to study the effects of **1** on L5-induced apoptosis in cultured ECs. In addition, we systematically examined the signaling pathways through which **1** prevents L5-induced apoptosis. Our findings suggest that treatment with **1** may be a novel approach to lowering the risk of or improving cardiovascular function in atherosclerosis-related disorders.



RESULTS AND DISCUSSION

Lipids are an essential component in the pathogenesis of atherosclerosis.²² The most electronegative subfraction of LDL, L5, induces vascular EC apoptosis, which is believed to promote the initiation and progression of atherosclerosis.^{12,15,21} We investigated the effects of **1** on plasma levels of L5 in Syrian hamsters, which develop atherosclerosis in a manner that closely mimics human pathology.^{23,24} Hamsters were fed a normal chow diet (control), a high-fat diet (HFD), or a HFD supplemented with the administration of 50 or 100 mg/kg of **1** via oral gavage (HFD+**1**) for 16 weeks ($n = 8$ per group). All hamsters in each group survived the entire length of the study (22 weeks). No significant differences were observed in body weight before the treatment period or after the treatment period at the end of the study (data not shown). We found that hamsters fed a HFD for 16 weeks had more electronegative LDL (Figure 1A) and a higher level of plasma L5 than did control hamsters fed a normal chow diet ($p < 0.01$, $n = 8$; Figure 1B and C). However, in hamsters fed a HFD in combination with receiving 50 or 100 mg/kg of **1** for 16 weeks, the electronegativity of LDL (Figure 1A) and the level of plasma L5 (Figure 1B and C) were significantly decreased in a manner dependent on the dose of **1** (50 mg/kg of **1**, $p < 0.05$; 100 mg/kg of **1**, $p < 0.01$, $n = 8$), indicating that the intake of **1** corresponded with a reduction in plasma L5 levels.

When we examined the levels of other lipids in the plasma of Syrian hamsters, we found that hamsters fed with a HFD had higher plasma concentrations of very-low-density lipoprotein cholesterol and triglyceride than did hamsters fed with a normal chow diet. In hamsters that were fed a HFD and supplemented with 50 or 100 mg/kg of **1**, plasma levels of total cholesterol, very-low-density lipoprotein cholesterol, LDL cholesterol, and triglyceride were reduced when compared with those levels in hamsters fed a HFD only ($p < 0.001$, Figure 2).

To study the effects of **1** on the development of atherosclerotic lesions in each group of hamsters, we used Oil Red O staining to examine lesion size in hamster aortas.

Because the aortic arch is a lesion-prone area for atherosclerosis,²⁵ we specifically examined lesion size from the aortic root to the mid-descending thoracic aorta. In hamsters fed with a HFD for 16 weeks, atherosclerotic lesion size was higher than that in the control group ($p < 0.001$, Figure 3A and B). However, the size of atherosclerotic lesions in hamsters fed a HFD was reduced by supplementation with 50 mg/kg of **1** (31.5% reduction, $p < 0.001$) or 100 mg/kg of **1** (47.3% reduction, $p < 0.001$) (Figure 3A and B). These results suggest that supplementation with **1** corresponded with a decrease in the size of atherosclerotic lesions.

Endothelial apoptosis is a very early step in atherogenesis.^{26–28} Because damage to ECs is prevented by antioxidants, the use of sesamol (**1**)—an antioxidant agent^{7,29}—may be a possible preventive treatment against EC damage that leads to atherosclerosis. To examine in vitro whether **1** can block EC apoptosis induced by L5, we treated human aortic endothelial cells (HAECs) with L5 (50 $\mu\text{g}/\text{mL}$) and increasing concentrations of **1** (0.3–3 μM) and examined apoptosis 24 h later by staining cells with Hoechst 33342 and calcein-AM. The results of fluorescence microscopy showed that, whereas L5 alone induced cell apoptosis ($p < 0.001$), the addition of **1** attenuated L5-induced cell apoptosis in a manner dependent on the dose of **1** (0.3 μM , $p < 0.01$; 1 and 3 μM , $p < 0.001$, Figure 4A). Moreover, many signaling proteins are involved in cell apoptosis, including caspases, which are essential for apoptosis (programmed cell death).³⁰ In cellular apoptosis pathways, caspase-3 is a frequently activated death protease that catalyzes the cleavage of several key cellular proteins.³¹ In all cell types examined, caspase-3 is indispensable for apoptotic chromatin condensation and DNA fragmentation, which are hallmarks of apoptosis.³² In a previous study, caspases were found to play a critical role in oxLDL-induced apoptosis in HAECs.³³ Using immunohistochemical analysis, we found that the expression of active caspase-3 in aortic sections from hamsters fed a HFD was reduced by supplementation with **1** (50 or 100 mg/kg, data not shown). Furthermore, when we examined caspase-3 activation in vitro, we found that **1** inhibited L5-induced caspase-3 activation in HAECs in a dose-dependent manner ($p < 0.001$, Figure 4B). These data indicate that L5-induced HAEC apoptosis is prevented by **1**.

To further investigate the mechanisms underlying the inhibitory effects of **1** on L5-induced EC apoptosis, we studied the effects of **1** on the cellular internalization of L5. The internalization of LDL is an early event in the apoptosis cascade.²¹

LOX-1 is a receptor for L5^{17,21} and ox-LDL.²¹ Although chemically different, L5 and oxLDL compete for entry into ECs through LOX-1.²¹ The binding of ox-LDL to LOX-1 induces several cellular events in ECs,³⁴ such as the activation of nuclear factor (NF)- κB , the upregulation of monocyte chemoattractant protein-1 (MCP-1) levels, and the reduction of intracellular nitric oxide levels.^{35,36} Accumulating evidence has indicated that LOX-1 is involved in endothelial dysfunction, inflammation, atherogenesis, myocardial infarction, vascular lipid retention under a hypertensive state, and intimal thickening after balloon catheter injury.^{21,37–39} The LOX-1 receptor internalizes L5 into ECs and macrophages, and increased expression of this receptor has been found in thrombi removed from the culprit coronary arteries of STEMI patients.⁴⁰ To monitor the internalization of L5 into ECs, we treated HAECs with 50 $\mu\text{g}/\text{mL}$ DiI-L5 and examined its uptake by using

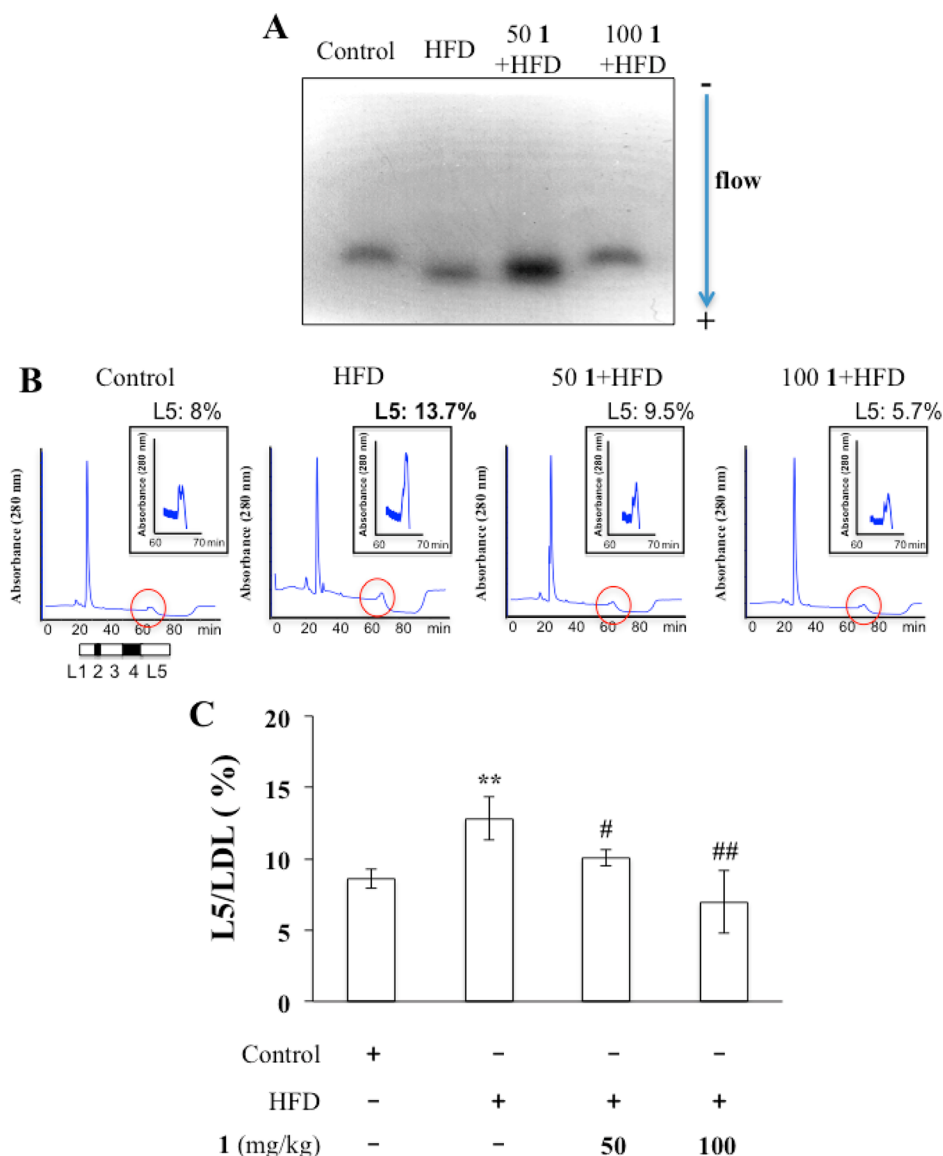


Figure 1. Inhibitory effects of **1** on the plasma elevation of L5 in Syrian hamsters fed with a high-fat diet (HFD). (A) Results of agarose gel electrophoresis showing the electronegativity of total LDL from hamsters fed a normal chow diet (control), a HFD, or a HFD supplemented with 50 or 100 mg/kg of **1** (50 1+HDF and 100 1+HDF, respectively). The arrow indicates the direction of electron flow. (B) Representative results of fast protein liquid chromatography showing the levels of plasma L5 (L5/LDL%) in hamsters fed a normal chow diet (control), a HFD, or a HFD supplemented with 50 or 100 mg/kg of **1** (50 1+HDF and 100 1+HDF, respectively). The red circles indicate the peak for L5. (C) Mean levels of plasma L5 (L5/LDL%) in the indicated groups of hamsters ($n = 8$). Bars represent standard deviation. ** $p < 0.01$ vs control group; # $p < 0.05$, ### $p < 0.01$ vs the HFD group. p -Values were determined by using the Wilcoxon rank-sum test.

fluorescence microscopy. At 30 min, DiI-L5 was visible in cells treated with DiI-L5 alone (Figure 5A). However, in cells pretreated with 3 μ M **1** for 30 min, L5 endocytosis via LOX-1 was blocked (Figure 5A). In addition, we found that the expression of LOX-1 was increased in HAECs treated with L5 ($p < 0.01$, Figure 5B) and not in cells treated with L1, but the pretreatment of HAECs with **1** inhibited the L5-induced expression of LOX-1 ($p < 0.001$, Figure 5B). These results suggest that **1** may block L5-induced apoptosis by reducing the internalization of L5 into ECs and attenuating the expression of LOX-1.

MAPK proteins transduce a large variety of external signals that lead to a wide range of cellular responses, including cell apoptosis. In mammals, three major MAPK pathways have been identified: ERK, JNK, and p38 MAPK. The p38 MAPK

pathway plays an essential role in cell apoptosis.⁴¹ The p38 MAPK protein provides a key signal that mediates the apoptosis of ECs induced by oxLDL.⁴² Therefore, we examined whether L5 also activates p38 MAPK and found that p38 MAPK phosphorylation was stimulated by the treatment of HAECs with L5 but not L1 in a time-dependent manner during the first 120 min ($p < 0.001$, Figure 6A). Moreover, we found that the pretreatment of cells with TS92 (a neutralizing antibody against LOX-1, 10 μ g/mL) blocked the L5-induced phosphorylation of p38 MAPK and activation of caspase-3 (Figure 6B and C). In addition, the pretreatment of cells with SB203580 (p38 MAPK inhibitor, 2 μ M) arrested L5-induced caspase-3 activation (Figure 6C). These results indicate that L5 induces the apoptosis of ECs via LOX-1/p38 MAPK/caspase-3 signaling. Importantly, in HAECs pretreated with **1**

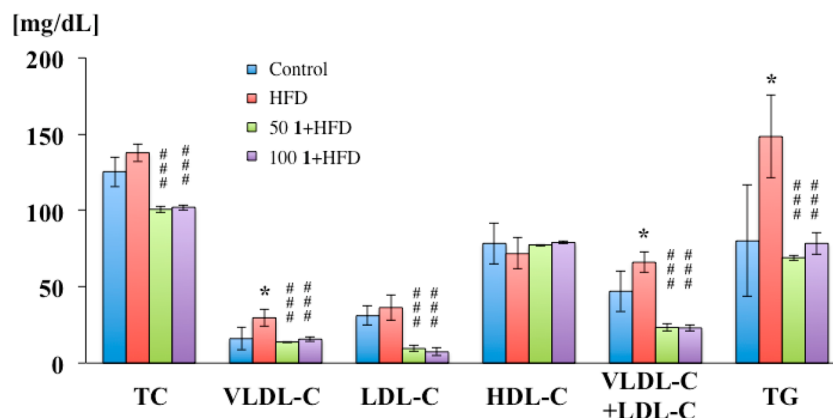


Figure 2. Effect of **1** on the concentration of plasma lipids in Syrian hamsters fed with various diets. Syrian hamsters were fed a normal chow diet (control), a high-fat diet (HFD), or a HFD supplemented with 50 mg/kg of **1** (50 1+HFD) or 100 mg/kg of **1** (100 1+HFD). Results are expressed as the mean \pm standard deviation ($n = 8$). p -Values were determined by using Student's t -test. * $p < 0.05$ vs the control group; ### $p < 0.001$ vs the HFD group. TC, total cholesterol; VLDL-C, very-low-density lipoprotein cholesterol; LDL-C, low-density lipoprotein cholesterol; HDL-C, high-density lipoprotein cholesterol; TG, triglyceride.

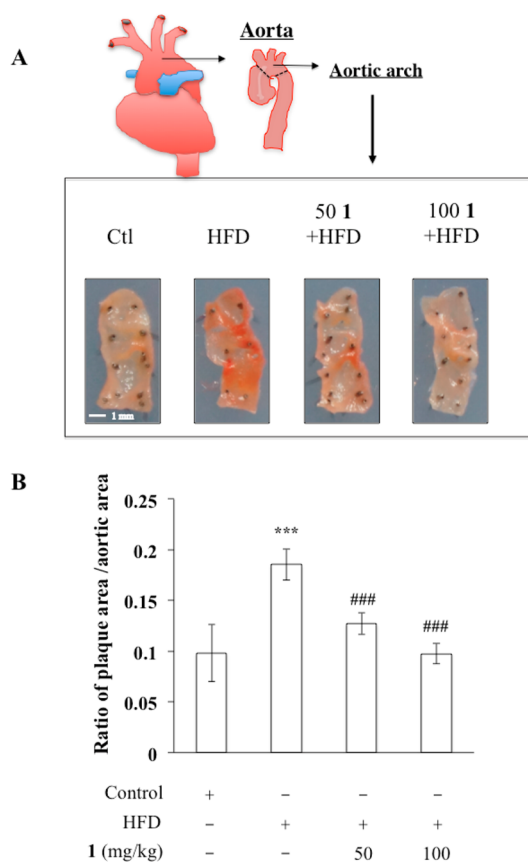


Figure 3. Reduction of atherosclerotic lesion size in Syrian hamsters fed a high-fat diet (HFD) supplemented with **1**. (A) Representative Oil Red O staining showing the end face luminal aortic surface (from the aortic root to the mid-descending thoracic aorta) in hamsters fed a normal chow diet (Ctl), a HFD, or a HFD supplemented with 50 mg/kg or 100 mg/kg of **1** (50 1+HFD and 100 1+HFD, respectively) for 16 weeks. Stained areas delineate lipid-rich lesions. Bar = 1 mm. (B) The atheroma area at 16 weeks in the indicated groups of hamsters ($n = 8$ per group). Data represent the mean ratio of plaque area over the total aortic luminal area and are expressed as the mean \pm standard deviation. p -Values were determined by using Student's t -test. *** $p < 0.001$ vs control group; ### $p < 0.001$ vs the HFD group.

(0.3–3 μ M), the L5-induced phosphorylation of p38 MAPK was significantly inhibited in a manner dependent on the dose of **1** ($p < 0.001$, Figure 6D). These findings suggest that **1** blocks the pro-apoptotic activation of p38 MAPK induced by L5 in HAECs. Furthermore, the inhibitory effects of **1** on the L5-induced phosphorylation of p38 MAPK and activation of caspase-3 were blocked by the pretreatment of HAECs with Wortmannin (PI3K inhibitor, 20 μ M), Akt inhibitor (2 nM), or L-NAME (inhibitor of nitric oxide synthase, 0.1 mM) ($p < 0.01$, Figure 6D–F), suggesting that PI3K/Akt/eNOS signaling is required for the inhibitory effect of **1** on the L5-induced phosphorylation of p38 MAPK and activation of caspase-3.

Akt and Akt-related serine-threonine kinases play important roles in signaling cascades that regulate cell survival, and the impairment of these signaling cascades has been implicated in the pathogenesis of degenerative disease.⁴³ Endothelial nitric oxide synthase (eNOS) is a target downstream of activated Akt⁴⁴ and plays a critical role in vascular function, including vascular signaling and remodeling, angiogenesis, and regulation of vascular tone.⁴⁵ When we examined the effects of **1** on the activation of eNOS and Akt, we found that **1** markedly increased their phosphorylation between 10 and 30 min in a time-dependent manner but decreased their phosphorylation between 60 and 240 min (Figure 7A and B). The pretreatment of HAECs with Wortmannin (20 nM) or Akt inhibitor (2 nM) inhibited the **1**-induced phosphorylation of Akt and eNOS at 30 min (Figure 7C and D), suggesting that **1** activates Akt/eNOS signaling, which may inhibit the pro-apoptotic L5-induced phosphorylation of p38 MAPK. In addition, using immunoblotting analysis, we confirmed our previously reported finding²¹ that Akt is dephosphorylated in HAECs treated with L5 (Figure 7E). However, when HAECs were pretreated with **1**, we found that **1** significantly reversed the dephosphorylation of Akt induced by L5 ($p < 0.01$, Figure 7E). In HAECs treated with a specific Akt inhibitor, we detected the activities of multiple signal transduction pathway elements downstream of the Akt pathway and found that **1** not only suppressed LOX-1-mediated, pro-apoptotic p38 MAPK/caspase-3 activation but also enhanced prosurvival PI3K/Akt/eNOS signaling. These findings are consistent with those previously showing that sesamol (**1**) upregulates eNOS signaling pathways.⁴⁶

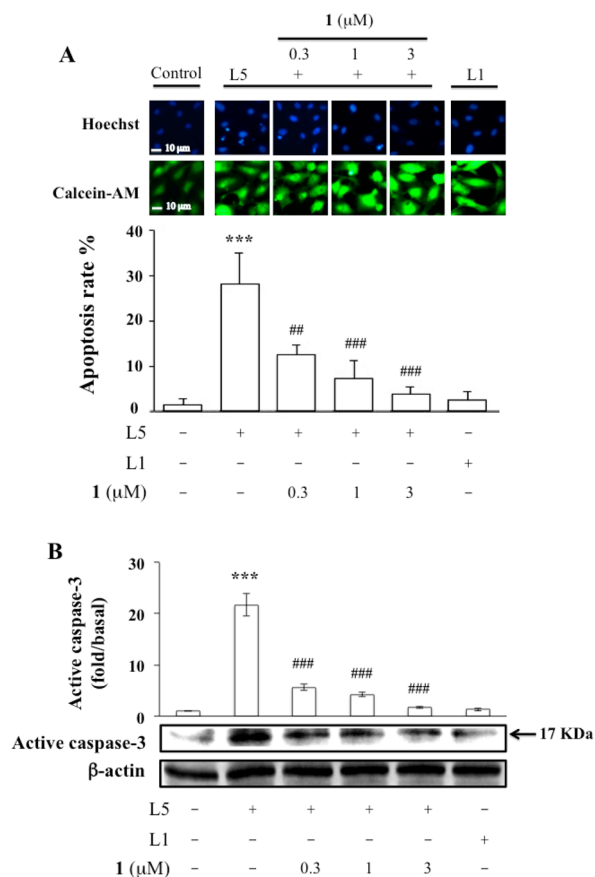


Figure 4. Effect of **1** on L5-induced apoptosis in human aortic endothelial cells (HAECs). HAECs were pretreated with vehicle (0.1% DMSO) or **1** (0.3, 1, or 3 μM) for 30 min and then incubated with or without 50 μg/mL L1 (control) or L5 for 24 h. (A) Epifluorescence microscopy images showing Hoechst 33342 staining (to assess nuclear morphology) and calcein-AM staining (to assess membrane integrity). HAECs with condensed, fragmented nuclei were considered to be undergoing apoptosis. Results are expressed as the mean percentage of cells undergoing apoptosis, evaluated in 6 samples of cells. Bars represent standard deviation. *p*-Values were determined by using Student's *t*-test. ****p* < 0.001 vs vehicle-treated group; ##*p* < 0.01, ###*p* < 0.001 vs L5-treated group. (B) Immunoblot analysis of activated caspase-3. Data were quantified by determining the optical density of bands. The bar graph shows the ratio of the expression of activated caspase-3 to that of β-actin (*n* = 4) relative to the vehicle-treated group, which was normalized to 1. Data are presented as the mean ± standard deviation. *p*-Values were determined by using Student's *t*-test. ****p* < 0.001 vs the vehicle-treated group; ###*p* < 0.001 vs the L5-treated group.

The major effect of lipid-lowering drugs is the reduction of elevated serum LDL cholesterol levels, which are believed to predispose individuals to atherosclerosis and its complications, acute myocardial infarction, cerebrovascular ischemic stroke, and peripheral disease. Given that **1** is a natural compound, it may be safer than lipid-lowering agents currently in clinical application. Moreover, recent studies have shown that a novel modified derivative of **1** (INV-430) can potently inhibit atherosclerotic plaque progression by reducing systemic and vascular oxidative stress and by reducing NF-κB activation via IKK2 inhibition.²⁹ In addition, **1** in the concentration range 2.5–100 μM inhibits platelet aggregation by increasing the rate of cyclic adenosine monophosphate (cAMP) formation and by attenuating NF-κB signaling events.^{10,47} Thus, **1** may be not

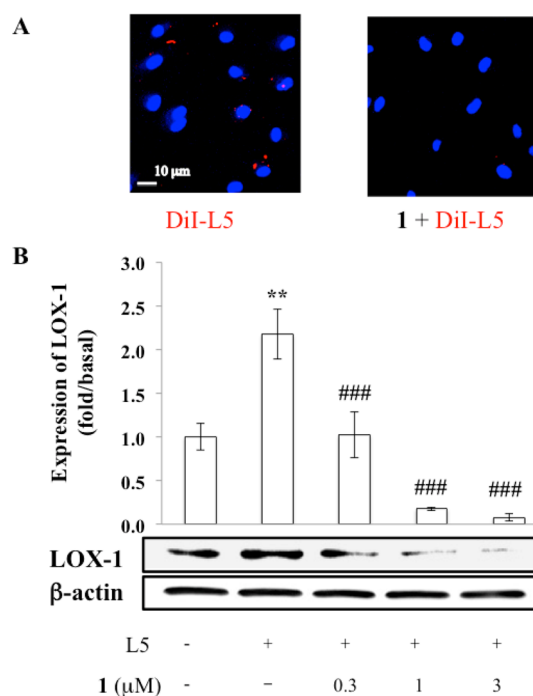


Figure 5. Inhibitory effects of **1** on the internalization of L5 by LOX-1 and the L5-induced expression of LOX-1 on human aortic endothelial cells (HAECs). (A) Fluorescence microscopy images showing the internalization of DiI-L5 in HAECs pretreated with or without 3 μM **1** for 30 min, followed by treatment with DiI-L5 (50 μg/mL) for 8 h (red = DiI-L5; blue = Hoechst 33342 nuclear staining; bar = 10 μm). (B) Immunoblot analysis showing the expression of LOX-1 in HAECs treated with or without the indicated concentration of **1** and L5 (50 μg/mL). Data are representative of 4 independent experiments. Data were quantified by determining the optical density of bands. The bar graph shows the ratio of the expression of LOX-1 to that of β-actin relative to the untreated control, which was normalized to 1. Data are presented as the mean ± standard deviation. *p*-Values were determined by using Student's *t*-test. ***p* < 0.01 vs the control untreated group; ###*p* < 0.001 vs the L5-treated group.

only an antioxidant, antiapoptotic, and lipid-lowering agent but also an antithrombotic and cardioprotective compound.

In summary, we have presented in vivo data showing that plasma L5 levels are reduced in Syrian hamsters administered with **1** and that atherogenic changes in the aortas of Syrian hamsters can be prevented by **1**. Furthermore, our in vitro data indicated that this antiatherogenic activity of **1** may be partly attributed to its ability to inhibit the L5-induced apoptosis of ECs, a key event in the development of atherosclerosis. These findings provide novel insight into a preventive role of **1** in the development of atherosclerosis and warrant additional studies regarding its potential use as a therapeutic agent.

EXPERIMENTAL SECTION

Chemicals and Antibodies. Sesamol (**1**) (5-hydroxy-1,3-benzodioxole; purity: 99.9% by GC) and Oil Red O were purchased from Sigma (St. Louis, MO, USA). Complete medium was purchased from Promo Cell (Heidelberg, Germany). Hoechst 33342 and calcein acetoxyethyl ester (calcein-AM) were purchased from Molecular Probes (Eugene, OR, USA). BCA protein assay reagents and SuperBlock blocking buffer were purchased from Pierce Biotechnology, Inc. (Rockford, IL, USA). Hybond-PVDF membrane was purchased from GE Healthcare Amersham (Buckinghamshire, UK). The monoclonal mouse antibody against phosphorylated p38 MAPK, monoclonal mouse antibody against p38 MAPK, polyclonal rabbit

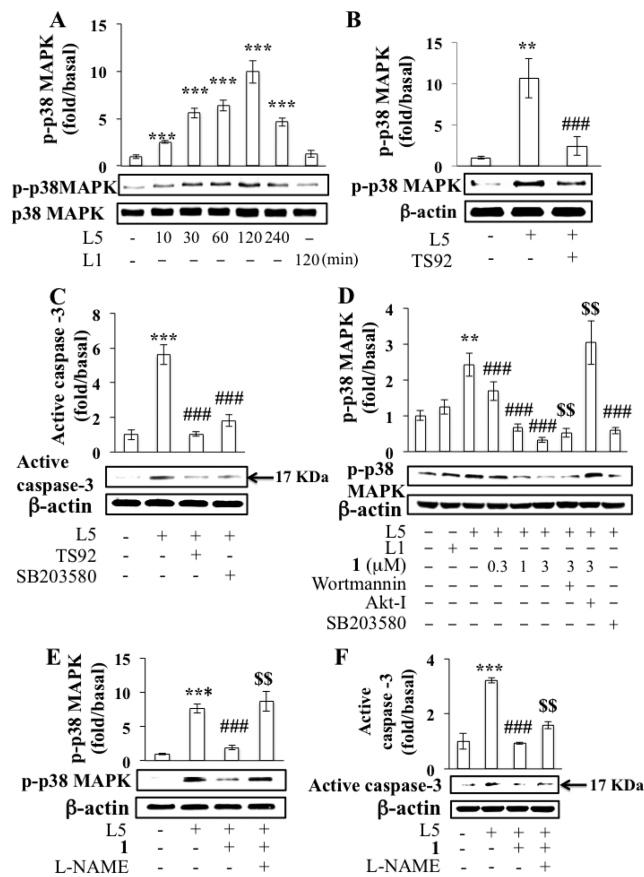


Figure 6. Effects of **1** on the L5-induced phosphorylation of p38 MAPK in human aortic endothelial cells (HAECs). (A) Levels of phosphorylated p38 (p-p38) MAPK are shown for HAECs treated with vehicle (0.1% DMSO) or with L5 (50 μg/mL) or L1 (50 μg/mL, control) for the indicated times (10, 30, 60, 120, or 240 min). The bar graph shows the expression of p-p38 MAPK at the indicated time point normalized to that in the vehicle-treated group. (B, D, E) Protein levels of p38 MAPK are shown for HAECs that were pretreated for 30 min with vehicle (0.1% DMSO), Wortmannin (20 nM), Akt inhibitor (Akt-I; 2 nM), or L-NAME (0.1 mM) before treatment with or without **1** (0.3, 1, or 3 μM) for 30 min or that were pretreated with TS92 (10 μg/mL) or SB2030580 (2 μM) for 30 min before treatment with or without L5 (50 μg/mL) or L1 (50 μg/mL; control) for 120 min. (C, F) Immunoblot analysis of activated caspase-3. HAECs were pretreated for 30 min with vehicle (0.1% DMSO) or L-NAME (0.1 mM) before treatment with or without **1** (3 μM) for 30 min or were pretreated with TS92 (10 μg/mL) or SB2030580 (2 μM) for 30 min, before treatment with or without L5 (50 μg/mL) for 24 h. Immunoblotting data are representative of 4 independent experiments. Data were quantified by determining the optical density of bands. The bar graph shows the ratio of the expression of p-p38 MAPK or active caspase-3 to that of p38 MAPK or β-actin, respectively, relative to the vehicle-treated control, which was normalized to 1. Data are expressed as the mean ± standard deviation and were compared by using Student's *t*-test. ***p* < 0.01, ****p* < 0.001 vs the vehicle-treated control group; ####*p* < 0.001 vs the L5-treated group; ^{ss}*p* < 0.01 vs the **1** (3 μM)- and L5-treated group.

antibody against cleaved (active) caspase-3, monoclonal mouse antibody against phosphorylated Akt, monoclonal mouse antibody against Akt, monoclonal rabbit antibody against phosphorylated eNOS, and polyclonal rabbit antibody against eNOS were purchased from Cell Signaling Technology (Beverly, MA, USA). The polyclonal rabbit antibody against LOX-1 was purchased from Biorbyt (Cambridgeshire, UK). The monoclonal mouse antibody against β-actin was purchased from Sigma. The secondary antirabbit or

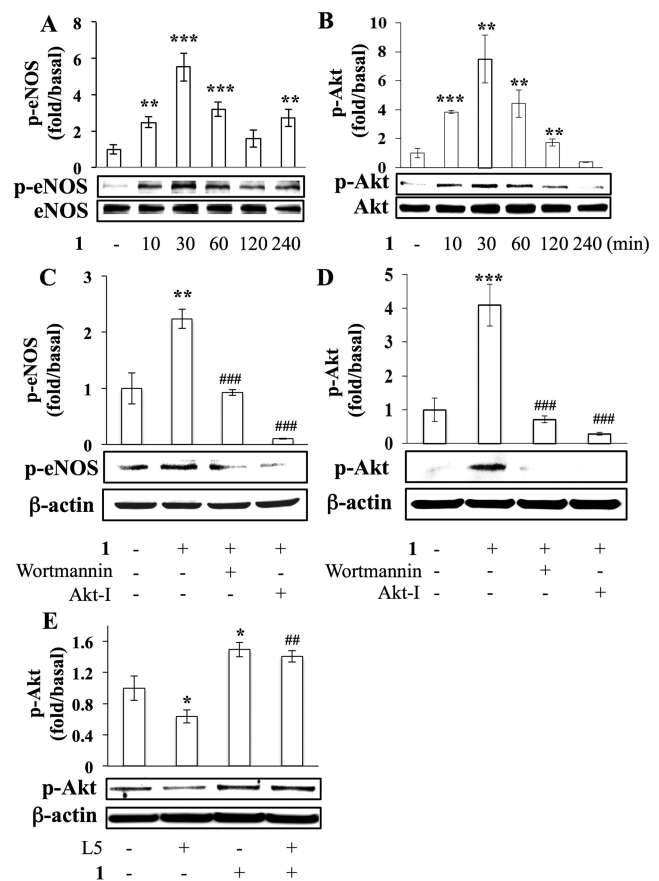


Figure 7. **1**-induced phosphorylation of eNOS and Akt in human aortic endothelial cells (HAECs). Time-course analysis of the effects of **1** (3 μM) on the phosphorylation of eNOS (A) and Akt (B) in HAECs. The supernatants of cell lysates were collected at different time points after treatment with vehicle (0.1% DMSO) or **1** (10, 30, 60, 120, and 240 min); the time course and treatments shown in A also apply to B. The effects of pretreating cells with vehicle, Wortmannin, or Akt-I on **1**-induced changes in eNOS (C) and Akt (D) phosphorylation. HAECs were pretreated for 30 min with vehicle (0.1% DMSO), 20 nM Wortmannin, or 2 nM Akt-I, followed by treatment with or without 3 μM of **1** for 30 min. (E) **1** significantly reversed the dephosphorylation of Akt by L5 in HAECs. HAECs were pretreated for 30 min with vehicle (0.1% DMSO) or 3 μM of **1**, followed by treatment with or without L5 (50 μg/mL) for 24 h. Western blot data are representative of 4 independent experiments. Data were quantified by determining the optical density of bands. The bar graphs show the ratio of the expression of p-eNOS to that of eNOS (A) or β-actin (C) and the ratio of the expression of p-Akt to that of Akt (B) or β-actin (D, E) relative to the respective vehicle-treated control, which was normalized to 1. Data are expressed as the mean ± standard deviation. *p*-Values were determined by using Student's *t*-test. **p* < 0.05, ***p* < 0.01, ****p* < 0.001 vs the vehicle-treated control group; ##*p* < 0.01 vs the L5-treated group; ###*p* < 0.001 vs the **1**-treated group.

antimouse IgG antibodies, Wortmannin, Akt inhibitor (Akt-I), SB2030580, and L-NAME were purchased from Santa Cruz Biotechnology (Dallas, TX, USA). ECL reagent was purchased from Millipore (Billerica, MA, USA). The lipophilic dye 1,1'-diiododecyl-3,3',3'-tetramethylindocarbocyanine perchlorate (DiI) was purchased from Invitrogen (Carlsbad, CA, USA). TS92 (human monoclonal antibody against LOX-1) was provided by the laboratory of Dr. Tatsuya Sawamura (National Cerebral and Cardiovascular Center, Japan).

Animal Experimental Protocol. Experiments involving hamsters were performed in accordance with the Guide for the Care and Use of Laboratory Animals, published by the U.S. National Institutes of Health (NIH Publication No. 85-23, revised 1996), and were performed as humanely as possible. All aspects of the animal care and animal procedures performed for this study were approved (permit no. CMU-102–263-C) by the China Medical University Animal Care and Use Committee (IACUC).

Thirty-two 6-week-old male Syrian hamsters were purchased from the National Laboratory Animal Center (NARLabs, Taipei, Taiwan) and individually housed in stainless-steel cages at 22 ± 4 °C on a 12 h light–dark cycle with free access to regular rodent chow and water. After 1 week of acclimatization, the hamsters were randomly divided into 4 experimental treatment groups ($n = 8$ hamsters each). For 16 weeks, group 1 was maintained on a normal chow diet only (control); group 2 was maintained on a high-fat diet only; and groups 3 and 4 were maintained on a HFD supplemented with 50 or 100 mg/kg of 1 (in 0.5% carboxymethyl cellulose [CMC] buffer solution; Sigma) per kg of body weight per day. The normal chow diet was a purified version of the AIN-93G diet with slight modifications and contained 13.9% (cal) fat. The HFD was a normal diet supplemented with 10% lard and 0.3% cholesterol and contained 60.0% (cal) fat. Diets were freshly mixed weekly in small amounts and stored at 0–4 °C to avoid spoilage. Sesamol (**1**) (Sigma) was administered by means of gavage in 0.5% CMC buffer solution. Hamsters in the HFD and control groups were administered 0.5% CMC buffer only. Food consumption and weight gain were measured daily and weekly, respectively. After the 16-week study period ended, the hamsters were anesthetized following a 12 h fast by inhalation of a mixture of 75% air and 25% O₂ gases containing 4% isoflurane. Blood samples were drawn from the inferior vena cava. Aortas and heart tissues were excised, rinsed with physiological saline, weighed, flash-frozen in liquid nitrogen, and stored at –80 °C until additional experiments were performed.

Biochemical Evaluation of Serum. Serum was separated from the blood by centrifugation at 3000g for 10 min. Serum levels of total cholesterol, triglyceride, very-low-density lipoprotein cholesterol, low-density lipoprotein cholesterol, and high-density lipoprotein cholesterol were determined by using commercial enzymatic kits with the SPOTCHEM™ EZ SP-4430 automated analyzer (ARKRAY, Inc., Kyoto, Japan).

LDL Isolation. To prevent contamination, blood samples were treated with 50 mU/mL aprotinin, 1% ampicillin/streptomycin, and 5 mM EDTA immediately after collection. Serum was obtained from whole blood by centrifugation at 1500 rpm for 15 min at 4 °C. LDL was isolated by using sequential potassium bromide density centrifugation to remove chylomicrons, very-low-density lipoprotein, and intermediate-density lipoprotein fractions, yielding LDL at a final density of 1.019 to 1.063 g/mL.¹² LDL was treated with 5 mM EDTA and nitrogen to avoid ex vivo oxidation.

Agarose Gel Electrophoresis. LDL samples (2.5 μg in 9 μL) were analyzed by using gel electrophoresis in 0.7% agarose (90 mM Tris and 90 mM boric acid, pH 8.2) at 100 V for 1.4 h, as previously described.⁴⁸

Subfractionation of LDL. Whole LDL was equilibrated by dialysis in a column loaded with buffer A (20 mM Tris-HCl [pH 8.0], 0.5 mM EDTA, 0.01% Na₃N₃). LDL was further divided into subfractions L1, L2, L3, L4, and L5 against a graded salt gradient by using anion-exchange columns (Uno-Q6; Bio-Rad Laboratories, Inc., Hercules, CA, USA) with the AKTA fast protein liquid chromatography system (GE Healthcare Life Science, Pittsburgh, PA, USA) as previously described.⁴⁸ The effluent was monitored at 280 nm and protected from ex vivo oxidation with 5 mM EDTA.¹⁷

Oil Red O Staining. We examined the presence of lipids in the aortic root to the mid-descending thoracic aorta. Tissues were stained with Oil Red O and counterstained with hematoxylin. Briefly, tissues were fixed with 4% paraformaldehyde for 10 min and washed twice with phosphate-buffered saline (PBS) at room temperature. The tissues were pretreated with 60% isopropyl alcohol for 5 min and then incubated with 0.6% (w/v) Oil Red O (Sigma) solution in 60% isopropyl alcohol for 30 min. Before use, the Oil Red O solution was

warmed to 55 °C and passed through a 0.22 μm filter. Tissues were then washed in running tap water for 2 min. For cross-sectional analysis, tissues were treated with hematoxylin for 1 min, and excess stain was removed with water. Images were obtained by using a stereoscope and were analyzed by using Image-Pro Plus software (Media Cybernetics, Rockville, MD, USA).^{22,49}

Cell Culture. Primary human aortic endothelial cells (PromoCell) were used for experiments after 3 or 4 passages and were maintained in complete medium (PromoCell) containing 2% fetal bovine serum with growth factor cocktail.

Apoptosis Assays. Subconfluent HAECs were pretreated with vehicle (0.1% DMSO) or **1** (0.3, 1, or 3 μM) for 30 min and incubated with or without L5 (50 μg/mL) for 24 h. L1 (50 μg/mL) was used as a negative control. Treated cells were stained for 10 min with 1 μM Hoechst 33342 (Molecular Probes) to assess nuclear morphology and with calcein acetoxyethyl ester (calcein-AM) (Molecular Probes) to assess membrane intensity. Fluorescence imaging was performed with an Olympus IX70 inverted microscope, and apoptotic cells were quantified as previously described.¹²

Labeling of L5 with 1,1'-Diiododecyl-3,3',3'-tetramethylindocarbocyanine Perchlorate. The lipophilic dye DiI (Invitrogen) was used to label L5 as described by Pitas and colleagues.⁵⁰ Briefly, L5 was diluted to 1 mg/mL with PBS and incubated with 80 μM DiI at 37 °C overnight. DiI-labeled L5 (DiI-L5) was then purified by using ultracentrifugation (density = 1.063 g/mL) and was subsequently dialyzed against PBS-EDTA (0.5 μM). During all steps, the mixture was protected from light. DiI-L5 was freshly prepared before use.

Monitoring of L5 Internalization by Using Fluorescence Microscopy. HAECs were pretreated with or without 3 μM **1** for 30 min, followed by the addition of DiI-L5 (50 μg/mL). To monitor the cellular internalization of DiI-L5, a Zeiss Axiovert 200 fluorescence microscope (Göttingen, Germany) was used to record the positions of DiI-L5 with respect to bright-field images in overlay.²¹

Signaling Pathway Analysis. Subconfluent HAECs were pretreated with vehicle (0.1% DMSO) or **1** (0.3, 1, or 3 μM) for 10, 30, 60, 120, or 240 min (for time-course analysis) or for 30 min and were then incubated with or without L5 (50 μg/mL) for 10, 30, 60, 120, and 240 min (for time-course analysis) or for 24 h. L1 (50 μg/mL) was used as a negative control. For experiments involving signaling pathway inhibitors, cells were pretreated for 30 min with Wortmannin (PI3K inhibitor, 20 nM), Akt inhibitor (2 nM), SB2030580 (2 μM; p38 MAPK inhibitor), L-NAME (nitric oxide synthase inhibitor, 0.1 mM), or TS92 (10 μg/mL, human monoclonal antibody against LOX-1). HAECs were analyzed by using Western blot analysis, as described below.

Western Blot Analysis. Cells were solubilized in NETN lysis buffer, and protein levels were measured by using the BCA protein assay (Pierce Biotechnology, Inc.). Cell lysates (50 μg each) were loaded onto a 10% sodium dodecyl sulfate (SDS) polyacrylamide gel, and proteins were separated by means of SDS polyacrylamide gel electrophoresis (SDS-PAGE). The separated proteins were transferred to a Hybond-P VDF membrane (GE Healthcare Amersham), followed by blocking with SuperBlock (Pierce Biotechnology, Inc.). For immunoblotting before and after treatments, membranes were incubated overnight at 4 °C with one of the following primary antibodies at a 1:1000 dilution: monoclonal mouse antibody against phosphorylated p38 MAPK, monoclonal mouse antibody against p38 MAPK, polyclonal rabbit antibody against cleaved (active) caspase-3, monoclonal mouse antibody against phosphorylated Akt, monoclonal mouse antibody against Akt, monoclonal rabbit antibody against phosphorylated eNOS, polyclonal rabbit antibody against eNOS (Cell Signaling Technology), polyclonal rabbit antibody against LOX-1 (Biorbyt), and monoclonal mouse antibody against β-actin (Sigma). Membranes were then incubated at room temperature for 30 min with secondary anti-rabbit or anti-mouse IgG antibodies conjugated to horseradish peroxidase at a 1:5000 dilution (Santa Cruz Biotechnology). Immunoreactive bands were detected by using ECL reagents (Millipore). Quantitative results were obtained by scanning reactive

bands and quantifying the optical density by using video densitometry (G-box Image System, Syngene, Frederick, MD, USA).⁵¹

Data Analysis and Statistical Procedures. The significance of the differences observed between groups was assessed by using Student's *t*-test. Probability values of $p < 0.05$ were considered significant. Results are expressed as the mean \pm standard deviation.

AUTHOR INFORMATION

Corresponding Authors

*(C.-H. Chen) E-mail: cchen@texasheart.org. Tel: 832-355-9026. Fax: 832-355-9333.

*(M.-Y. Shen) E-mail: shenmy1124@gmail.com. Tel: +886-4-22052121, ext. 7502.

Author Contributions

#W.-Y. Chen and F.-Y. Chen contributed equally to this work.

Notes

The authors declare no competing financial interest.

ACKNOWLEDGMENTS

The authors thank N. Stancel, of the Texas Heart Institute in Houston, Texas, for editorial assistance. This work was supported by grants from the American Diabetes Association (1-04-RA-13); the National Institutes of Health (HL-63364); the National Science Council of Taiwan (NSC102-2320-B-039-058 and NSC100-2314-B-039-040-MY3); National Health Research Institutes of Taiwan (NHRI-EX103-10305SI and NHRI-EX104-10305SI); Taiwan Ministry of Health and Welfare Clinical Trial and Research Center of Excellence (MOHW103-TDU-B-212-113002 and MOHW104-TDU-B-212-113002); Stroke Biosignature Project Grant of Academia Sinica, Taiwan (BM101100888, BM102021169, BM103010096, and BM104010092); China Medical University, Taiwan (CMU102-N-02 and CMU103-N-08); China Medical University Hospital, Taiwan (DMR-102-091); China Medical University under the "Aim for the Top University Plan" of the Ministry of Education, Taiwan; and Kaohsiung Medical University, Taiwan ("Aim for the Top Universities Grant", KMU-TP103D03).

REFERENCES

- Guyton, J. R.; Slee, A. E.; Anderson, T.; Fleg, J. L.; Goldberg, R. B.; Kashyap, M. L.; Marcovina, S. M.; Nash, S. D.; O'Brien, K. D.; Weintraub, W. S.; Xu, P.; Zhao, X. Q.; Boden, W. E. *J. Am. Coll. Cardiol.* **2013**, *62*, 1580–1584.
- Gupta, N. K.; Lewis, J. H. *Aliment. Pharmacol. Ther.* **2008**, *28*, 1021–1041.
- Kiortsis, D. N.; Filippatos, T. D.; Mikhailidis, D. P.; Elisaf, M. S.; Liberopoulos, E. N. *Atherosclerosis* **2007**, *195*, 7–16.
- Auger, C.; Caporiccio, B.; Landrault, N.; Teissedre, P. L.; Laurent, C.; Cros, G.; Besancon, P.; Rouanet, J. M. *J. Nutr.* **2002**, *132*, 1207–1213.
- Afonso, M. S.; de, O. S. A. M.; Carvalho, E. B.; Rivelli, D. P.; Barros, S. B.; Rogero, M. M.; Lottenberg, A. M.; Torres, R. P.; Mancini-Filho, J. *Nutr. Metab. (London)* **2013**, *10*, 19.
- Fukuda, Y.; N, M.; Osawa, T.; Namiki, M. *J. Am. Oil Chem. Soc.* **1986**, *63*, 5.
- Kaur, I. P.; Saini, A. *Mutat. Res.* **2000**, *470*, 71–76.
- Kapadia, G. J.; Azuine, M. A.; Tokuda, H.; Takasaki, M.; Mukainaka, T.; Konoshima, T.; Nishino, H. *Pharmacol. Res.* **2002**, *45*, 499–505.
- Sharma, S.; Kaur, I. P. *Int. J. Dermatol.* **2006**, *45*, 200–208.
- Chang, C. C.; Lu, W. J.; Chiang, C. W.; Jayakumar, T.; Ong, E. T.; Hsiao, G.; Fong, T. H.; Chou, D. S.; Sheu, J. R. *J. Nutr. Biochem.* **2010**, *21*, 1214–1221.
- Ross, R.; Harker, L. *Science* **1976**, *193*, 1094–1100.

(12) Chen, C. H.; Jiang, T.; Yang, J. H.; Jiang, W.; Lu, J.; Marathe, G. K.; Pownall, H. J.; Ballantyne, C. M.; McIntyre, T. M.; Henry, P. D.; Yang, C. Y. *Circulation* **2003**, *107*, 2102–2108.

(13) Lewis, J. C.; Kottke, B. A. *Science* **1977**, *196*, 1007–1009.

(14) Huynh, J.; Nishimura, N.; Rana, K.; Peloquin, J. M.; Califano, J. P.; Montague, C. R.; King, M. R.; Schaffer, C. B.; Reinhart-King, C. A. *Sci. Transl. Med.* **2011**, *3*, 112–122.

(15) Avogaro, P.; Bon, G. B.; Cazzolato, G. *Arteriosclerosis* **1988**, *8*, 79–87.

(16) Wang, G.-J.; Chang, C.-T.; Yang, C.-Y.; Chen, C.-H. *Biomed. Pharmacother.* **2012**, *2*, 147–154.

(17) Chan, H. C.; Ke, L. Y.; Chu, C. S.; Lee, A. S.; Shen, M. Y.; Cruz, M. A.; Hsu, J. F.; Cheng, K. H.; Lu, J.; Lai, W. T.; Sawamura, T.; Sheu, S. H.; Yen, J. H.; Chen, C. H. *Blood* **2013**, *122*, 3632–3641.

(18) Lu, J.; Jiang, W.; Yang, J. H.; Chang, P. Y.; Walterscheid, J. P.; Chen, H. H.; Marcelli, M.; Tang, D.; Lee, Y. T.; Liao, W. S.; Yang, C. Y.; Chen, C. H. *Diabetes* **2008**, *57*, 158–166.

(19) Chen, C. H.; Dixon, R. A.; Ke, L. Y.; Willerson, J. T. *Circ. Res.* **2009**, *104*, 1038–1040.

(20) Lee, A. S.; Wang, G. J.; Chan, H. C.; Chen, F. Y.; Chang, C. M.; Yang, C. Y.; Lee, Y. T.; Chang, K. C.; Chen, C. H. *Apoptosis* **2012**, *17*, 1009–1018.

(21) Lu, J.; Yang, J. H.; Burns, A. R.; Chen, H. H.; Tang, D.; Walterscheid, J. P.; Suzuki, S.; Yang, C. Y.; Sawamura, T.; Chen, C. H. *Circ. Res.* **2009**, *104*, 619–627.

(22) Kim, S.-H.; Lee, E.-S.; Lee, J. Y.; Lee, E. S.; Lee, B.-S.; Park, J. E.; Moon, D. W. *Circ. Res.* **2010**, *106*, 1332–1341.

(23) Ohtani, H.; Hayashi, K.; Hirata, Y.; Dojo, S.; Nakashima, K.; Nishio, E.; Kurushima, H.; Saeki, M.; Kajiyama, G. *J. Lipid Res.* **1990**, *31*, 1413–1422.

(24) Nistor, A.; Bulla, A.; Filip, D. A.; Radu, A. *Atherosclerosis* **1987**, *68*, 159–173.

(25) Zhao, Y.; Pennings, M.; Hildebrand, R. B.; Ye, D.; Calpe-Berdiel, L.; Out, R.; Kjerrulf, M.; Hurt-Camejo, E.; Groen, A. K.; Hoekstra, M.; Jessup, W.; Chimini, G.; Van Berkel, T. J. C.; Van Eck, M. *Circ. Res.* **2010**, *107*, e20–e31.

(26) Weber, C.; Noels, H. *Nat. Med.* **2011**, *17*, 1410–1422.

(27) Davignon, J.; Ganz, P. *Circulation* **2004**, *109*, III27–III32.

(28) Vanhoutte, P. M. *Circ. J.* **2009**, *73*, 595–601.

(29) Ying, Z.; Kherada, N.; Kampfrath, T.; Mihai, G.; Simonetti, O.; Desikan, R.; Selvendiran, K.; Sun, Q.; Ziouzenkova, O.; Parthasarathy, S.; Rajagopalan, S. *Arterioscler. Thromb. Vasc. Biol.* **2011**, *31*, 536–542.

(30) Peter, M. E. *Nature* **2011**, *471*, 310–312.

(31) Li, L. Y.; Luo, X.; Wang, X. *Nature* **2001**, *412*, 95–99.

(32) Porter, A. G.; Janicke, R. U. *Cell Death Differ.* **1999**, *6*, 99–104.

(33) Chen, J.; Mehta, J. L.; Haider, N.; Zhang, X.; Narula, J.; Li, D. *Circ. Res.* **2004**, *94*, 370–376.

(34) Kume, N.; Murase, T.; Moriwaki, H.; Aoyama, T.; Sawamura, T.; Masaki, T.; Kita, T. *Circ. Res.* **1998**, *83*, 322–327.

(35) Neri Serneri, G. G.; Coppo, M.; Bandinelli, M.; Paoletti, P.; Toscano, T.; Micalizzi, E.; Chiostrri, M.; Boddi, M. *Atherosclerosis* **2013**, *226*, 476–482.

(36) Li, D.; Mehta, J. L. *Circulation* **2000**, *101*, 2889–2895.

(37) Li, D.; Williams, V.; Liu, L.; Chen, H.; Sawamura, T.; Antakli, T.; Mehta, J. L. *Am. J. Physiol. Heart Circ. Physiol.* **2002**, *283*, H1795–H1801.

(38) Nakano, A.; Inoue, N.; Sato, Y.; Nishimichi, N.; Takikawa, K.; Fujita, Y.; Kakino, A.; Otsui, K.; Yamaguchi, S.; Matsuda, H.; Sawamura, T. *J. Hypertens.* **2010**, *28*, 1273–1280.

(39) Morawietz, H. *Dtsch. Med. Wochenschr.* **2010**, *135*, 308–312.

(40) Chang, K.-C.; Wang, Y.-C.; Chang, S.-S.; Lo, P.-H.; Lu, J.; Sawamura, T.; Lee, Y.-T.; Burns, A. R.; Chen, C.-H. *Circulation* **2012**, *126*, A13127.

(41) Perfettini, J.-L.; Castedo, M.; Nardacci, R.; Ciccocanti, F.; Boya, P.; Roumier, T.; Larochette, N.; Piacentini, M.; Kroemer, G. *J. Exp. Med.* **2005**, *201*, 279–289.

(42) Takahashi, M.; Okazaki, H.; Ogata, Y.; Takeuchi, K.; Ikeda, U.; Shimada, K. *Atherosclerosis* **2002**, *161*, 387–394.

- (43) Franke, T. F.; Kaplan, D. R.; Cantley, L. C. *Cell* **1997**, *88*, 435–437.
- (44) Fulton, D.; Gratton, J. P.; McCabe, T. J.; Fontana, J.; Fujio, Y.; Walsh, K.; Franke, T. F.; Papapetropoulos, A.; Sessa, W. C. *Nature* **1999**, *399*, 597–601.
- (45) Atochin, D. N.; Wang, A.; Liu, V. W.; Critchlow, J. D.; Dantas, A. P.; Looft-Wilson, R.; Murata, T.; Salomone, S.; Shin, H. K.; Ayata, C.; Moskowitz, M. A.; Michel, T.; Sessa, W. C.; Huang, P. L. *J. Clin. Invest.* **2007**, *117*, 1961–1967.
- (46) Chen, P. R.; Tsai, C. E.; Chang, H.; Liu, T. L.; Lee, C. C. *Lipids* **2005**, *40*, 955–961.
- (47) Chang, C. C.; Lu, W. J.; Ong, E. T.; Chiang, C. W.; Lin, S. C.; Huang, S. Y.; Sheu, J. R. *J. Biomed. Sci.* **2011**, *18*, 93.
- (48) Yang, C. Y.; Raya, J. L.; Chen, H. H.; Chen, C. H.; Abe, Y.; Pownall, H. J.; Taylor, A. A.; Smith, C. V. *Arterioscler. Thromb. Vasc. Biol.* **2003**, *23*, 1083–1090.
- (49) Sahara, M.; Ikutomi, M.; Morita, T.; Minami, Y.; Nakajima, T.; Hirata, Y.; Nagai, R.; Sata, M. *Cardiovasc. Res.* **2014**, *101*, 236–246.
- (50) Pitas, R. E.; Innerarity, T. L.; Weinstein, J. N.; Mahley, R. W. *Arteriosclerosis* **1981**, *1*, 177–185.
- (51) Shen, M. Y.; Liu, C. L.; Hsiao, G.; Liu, C. Y.; Lin, K. H.; Chou, D. S.; Sheu, J. R. *Planta Med.* **2008**, *74*, 1240–1245.